Scaling and vortex dynamics after the quench of a system with a continuous symmetry

M. Mondello and Nigel Goldenfeld
Department of Physics and Materials Research Laboratory, University of Illinois at Urbana-Champaign, 1110 West Green Street, Urbana, Illinois 61801
(Received 27 June 1990)

We study the dynamics of a system with a nonconserved complex order parameter, following a deep quench. In contrast to the case when the order parameter has a discrete symmetry, we observe an effective value of the dynamical exponent at early times of $\phi=0.375\pm0.005$. In this regime, finite-size scaling of the scattering function is observed. At later times, we observe a crossover to $\phi=0.5\pm0.02$. Our results indicate that any renormalization of the kinetic coefficient must be small.

I. INTRODUCTION

The ordering dynamics of a physical system after a deep quench below its transition point is believed to depend upon the dimension of the system, its internal symmetry group, and the presence of conservation laws.[1] During spinodal decomposition of a binary alloy, for example, the system proceeds to its final state of two-phase coexistence through the development of a pattern characterized by a single time-dependent length scale λ. It has been found that λ varies with time t according to $\lambda(t)\sim t^{\phi}$, where the dynamical exponent $\phi=1/3$ for the case of a conserved order parameter and $\phi=1/2$ for the case of a nonconserved order parameter.[2,3] These results do not seem to depend upon the dimension D of the system. Furthermore, the dynamical scattering function is found to obey a scaling law:

$$S(k,t)=\lambda(t)^{D}\Phi(k\lambda(t)) . \tag{1.1}$$

The purpose of this paper is to investigate the dynamics of the phase transition when the Hamiltonian has a continuous rather than a discrete symmetry. Although the low-temperature phase is unique when the Hamiltonian has a continuous symmetry, the phenomenological description of the approach to equilibrium should not differ from that in the case of the discrete symmetry; in both cases, the order-parameter evolution is determined by the chemical potential. We are interested in the following questions: (i) If the order-parameter symmetry is continuous rather than discrete, the system cannot support the domain walls that are believed to be responsible for the power laws,[3] observed in systems with a discrete symmetry. How, then, are the scaling laws changed in a system with a continuous symmetry? (ii) How do the defects present in the case of a continuous symmetry affect the dynamics after a quench?

Previous studies have concentrated on systems whose effective Hamiltonian has O(n) symmetry. Mazenko and Zannetti,[4] and de Pasquale and Tartaglia[5] have considered the $n=\infty$ case. Both papers find a Gaussian form for the scaling function $\Phi(x)$ and an exponent $\phi=1/2$. Toyoki and Honda[6] studied the complex nonconserved order-parameter case in $D=3$ using the defect dynamics picture proposed by Kawasaki.[7] Also in this case it was found that $\phi=1/2$. Nishimori and Nukii[8] have studied numerically the dynamics of line defects in the same system ($n=2$, $D=3$). They found that the length of defect line decreases with time as $l(t)\sim t^{-0.75\pm0.05}$. A molecular-dynamics study[9] of annihilating vortex points in $D=2$ is consistent with a dynamical exponent $\phi=1/2$.

More recently, Bray[10] has proposed a general argument to predict ϕ for the conserved order-parameter case using an analogy with critical dynamics. In his argument, the long-time behavior of the system is controlled by a zero-temperature fixed point, whose characteristics do not differ significantly from the Wilson-Fisher fixed point, which controls the critical dynamics of model B.[11] In particular, the absence of renormalization of the kinetic coefficient M is justified[12] by using the conventional argument valid for the critical dynamics of model B. Bray's argument has been criticized[13] in the case $n=1$ for not properly taking into account the domain walls. Goldenfeld and Oono[13] have argued that one of the effects of the domain walls is to introduce a renormalization of the kinetic coefficient in the conserved case but not in the case of a nonconserved order parameter. This result, if correct, would be quite different from the situation in critical dynamics. In principle, then, one of the key assumptions of Bray's argument could be tested, if it can be determined whether or not the kinetic coefficient is renormalized in the nonconserved case. For $n\geq2$, when there are no domain walls, the criticism of Goldenfeld and Oono does not seem to apply, and the argument may be extended to the nonconserved case to give $\phi=1/2$, $n\geq2$, $D=2$. In making this naive extension, we have assumed that it is not necessary to renormalize the kinetic coefficient.[12] Any renormalization of the kinetic coefficient would give a value for ϕ different from 1/2. We will find that our numerical simulations are consistent with the value $\phi=0.5\pm0.02$, implying that the renormalization of the kinetic coefficient, if present, must be very small. In contrast, the critical dynamics of model A does require a renormalization of the kinetic coefficient.

We have performed numerical simulations of a system

with a nonconserved order parameter[14] in $D=2$ whose effective Hamiltonian has O(n) symmetry, with $n=2$. Such a system relaxes to equilibrium not only through the dynamics of Goldstone modes, but also through the annihilation of vortices. Although our principal motivation in studying this problem was to test Eq. (1.1) we have found that at early times the vortex distribution relaxes anomalously slowly: $\phi<1/2$, a result which we have been able to relate to the subdiffusive character of the initial motion of the vortices. This behavior is a transient, because at long times, the exponent ϕ crosses over to a larger value of $\phi=0.5\pm0.02$; of course, we cannot exclude the possibility that some new behavior might arise at an even later time. We emphasize that these results constrast with the behavior observed in simulations with a scalar order parameter. A direct numerical study of the dynamical evolution of the domain boundaries (the characteristic defects in a system with discrete symmetry) indicated that, for a critical quench, the 1/2 exponent is satisfied from early times.[15] We have also made an extensive study of the scaling of the correlation functions of this system, and have observed a finite-size scaling of the scattering function of Eq. (1.1). We also observed scaling behavior of the real-space correlation function of the order parameter and of the vortex-vortex correlation functions. In all cases, the scaling behavior is obeyed even when ϕ has not yet reached its final value.

In Sec. II we introduce our model and describe some of the qualitative features of the dynamics. Section III is devoted to a quantitative analysis of the relaxation dynamics in terms of a typical time-dependent length scale. In this section we compare four possible choices for the characteristic length scale and discuss the results for the power-law exponent ϕ. We then discuss, in Sec. IV, the vortex motion on the lattice. In Sec. V we consider the dynamical scaling behavior of real-space and momentum-space correlation functions, including finite-size scaling. We make a few final remarks and summarize our conclusions in Sec. VI.

During the final drafting of this paper we have received unpublished work by Newman, Bray and Moore.[16] They investigated analytically and numerically the relaxation of vector spin systems ($2\le n\le 5$) in $D=1$. For $n=2$ they find a Gaussian scaling function and an exponent $\phi=1/4$. Using a one-dimensional version of the model introduced in Sec. II we have been able to confirm their findings.

II. MODEL

We consider a complex ($n=2$), nonconserved order-parameter field on a $L\times L$ lattice in two dimensions; a physical realization might be the ferromagnetic transition of a planar ferromagnet in two dimensions. The evolution of the order-parameter field $\Psi(\mathbf{r},t)\equiv X(\mathbf{r},t)+iY(\mathbf{r},t)$ is governed by the same phenomenological equation as in the case of a system with a discrete symmetry:

$$\frac{\partial\Psi(\mathbf{r},t)}{\partial t}=-M\frac{\partial F(\Psi(\mathbf{r},t))}{\partial\Psi^*(\mathbf{r},t)}\ , \tag{2.1}$$

where M is a kinetic coefficient, assumed to be independent of Ψ and

$$F\{\Psi(\mathbf{r},t)\}=\int d^2\mathbf{r}\left[|\nabla\Psi(\mathbf{r},t)|^2-a|\Psi(\mathbf{r},t)|^2+\frac{b}{2}|\Psi(\mathbf{r},t)|^4\right]. \tag{2.2}$$

The coefficients a and b are positive after the quench. We performed our simulations using a cell-dynamics scheme, a computationally efficient coarse-grained description of the ordering dynamics.[17] The evolution of the system is controlled, in our case, by the local (on-site) nonlinear relaxation process and isotropic Laplacian averaging, which couples nearest-neighbor ($\langle$NN$\rangle$) and next-nearest-neighbor ($\langle$NNN$\rangle$) sites. The corresponding equations in terms of the $X(\mathbf{r},t)$ and $Y(\mathbf{r},t)$ fields read

$$\begin{aligned}X(\mathbf{n},t+1)&=A\tanh[R(\mathbf{n},t)][X(n,t)/R(\mathbf{n},t)]\\&\quad+C[\langle\langle X(\mathbf{n},t)\rangle\rangle-X(\mathbf{n},t)]\ ,\\Y(\mathbf{n},t+1)&=A\tanh[R(\mathbf{n},t)][Y(\mathbf{n},t)/R(\mathbf{n},t)]\\&\quad+C[\langle\langle Y(\mathbf{n},t)\rangle\rangle-Y(\mathbf{n},t)]\ ,\end{aligned} \tag{2.3}$$

where $R(\mathbf{n},t)=|\Psi(\mathbf{n},t)|$ and

$$\langle\langle\psi(\mathbf{n},t)\rangle\rangle\equiv\sum_{\langle\mathrm{NN}\rangle}\left[\frac{\psi(\mathbf{m},t)}{6}\right]+\sum_{\langle\mathrm{NNN}\rangle}\left[\frac{\psi(\mathbf{m},t)}{12}\right]. \tag{2.4}$$

Here $\mathbf{n}$ and $\mathbf{m}$ represent the lattice sites, A gives a measure of the depth of the quench, and C controls the coupling strength. The unit of time is implicitly defined in terms of A and C. For our simulations we apply periodic boundary conditions and choose $A=1.3$ and $C=0.5$. These parameters describe the system after the quench ($A>1$), when the initial high-temperatures configuration of the order-parameter field becomes unstable, and the system relaxes to one of its new (infinitely degenerate) equilibrium configurations. The initial values of the vector components of Ψ are randomly chosen to be between -0.1 and 0.1 of their final equilibrium length (~1). Thus, initially, the relative orientations of the vectors are random (uncorrelated) and the average number of vortices (on a square lattice) is equal to 1/3 the number of lattices sites.[18]

The growth of the order parameter on the coupled-lattice sites is slower than it would be on isolated sites ($C=0$), because of the initial high vortex density. After about 30 time steps, over 98% of the vortices have annihilated and most vectors, outside the vortex cores, have reached their equilibrium length. A qualitative analysis of the subsequent evolution of the system already indicates the presence of a characteristic time-independent vortex-core size (ξ), analogous to the domain-wall thickness of the Ising case ($n=1$), and of a single-vortex field configuration extending around each vortex core up to distances comparable with the average time-dependent intervortex spacing (defined below).

III. DYNAMICS AND POWER-LAW BEHAVIOR

We now turn to a detailed discussion of the dynamics. There are several *a priori* independent characteristic

length scales in the system. The first two moments ($\bar{k}_1$ and $\bar{k}_2$) of $S(k,t)$, the circularly averaged time-dependent scattering function,[19]

$$\bar{k}_m(t)=\frac{\int_0^\infty dk\, k^m S(k,t)}{\int_0^\infty dk\, k^{m-1} S(k,t)}, \quad m=1,2\ , \tag{3.1}$$

define two characteristic lengths scales, $\lambda_m(t)=L/(2\pi\bar{k}_m(t))$, $m=1,2$. Alternatively, we can use the average intervortex spacing defined as $d(t)=L/\sqrt{N(t)}$, where $N(t)$ is the number of vortices remaining at time t. There is also a characteristic length associated with the real-space correlation function of the order parameter

$$C(r,t)\equiv\frac{\langle\Psi^*(r,t)\Psi(0,t)\rangle}{\langle\Psi^*(0,t)\Psi(0,t)\rangle}\ ,$$

namely, the halfwidth of the main peak of the correlation function $r_{1/2}(t)$ defined by the relation $C(r_{1/2}(t),t)=1/2$.

Within statistical error, in the time interval considered ($100\le t\le 6400$), $\lambda_2(t)/d(t)=1.88(\pm.02)$; this ratio is not only independent of time, but is also independent of the system size,[20] as can be seen from the inset of Fig. 1. In the main body of the figure we plot the two length scales against each other. The corresponding ranges of variation are in units of a lattice spacing.

We have investigated the expected power-law decay for $\bar{k}_m(t)\propto t^{-\phi}$ and $N(t)\propto t^{-2\phi}$. Our results indicate that for $\bar{k}_2$, over the time range considered, there is a small but measurable deviation from a simple power-law behavior. Initially, $\phi=\frac{1}{8}(\pm 0.005)$, but at later times the exponent is closer to 0.5 ± 0.02, as shown in Fig. 2.[21] New effects seem to appear toward the end of the run (see Sec. IV) but statistical uncertainties at this late stage prevent us from reaching a definitive conclusion about the asymptotic value of ϕ. These results are in sharp contrast to earlier findings for the discrete symmetry case,[17] where no such effects are observed. It should be pointed out, however, that in the scalar order-parameter case, the $\bar{k}_2$ moment of the scattering function was not considered since it diverges in the thermodynamic limit, due to the sharpness of the interface (Porod's law).[22]

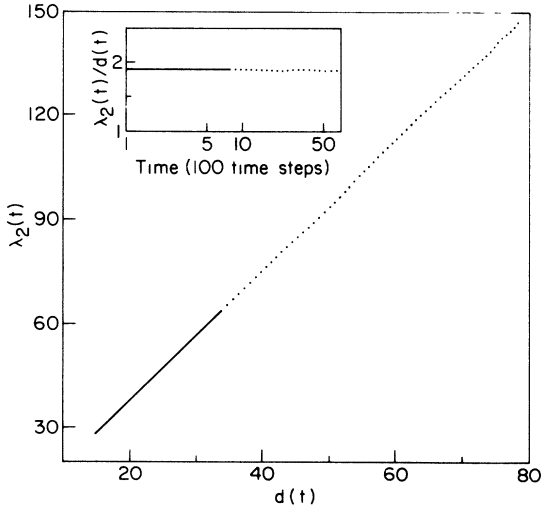

FIG. 1. Graph of $\lambda_2(t)$ vs $d(t)$ (see main text for definitions and units). In the inset is shown a plot of the ratio of $\lambda_2(t)/d(t)$ vs time (on a logarithmic scale) in units of 100 time steps. The dotted line is a linear interpolation of the data points taken on 512×512 lattices (averaged over 28 initial conditions) and the (superimposed) solid line interpolates data taken on 256×256 lattices (averaged over 60 initial conditions).

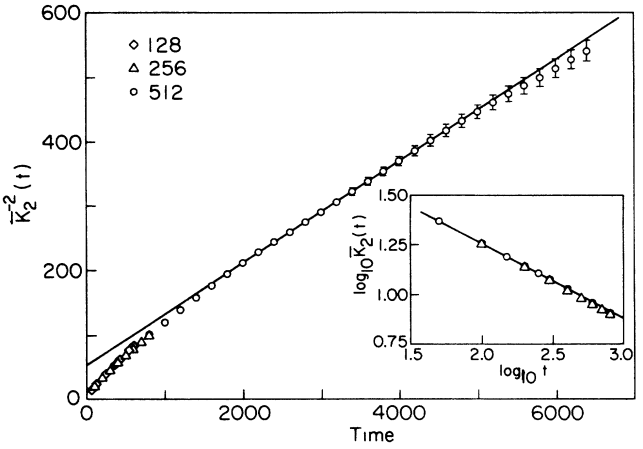

FIG. 2. Inverse of average wave-number square $\bar{k}_2^{-2}$ vs t. A straight line is drawn for comparison. In the inset is shown the graph of $\log_{10}(\bar{k}_2)$ vs $\log_{10}(t)$ in the time interval ($50\le t\le 800$). The solid line in the inset has a slope of $-3/8$. ○ corresponds to data taken on 512×512 lattices (averaged over 28 initial conditions), △ corresponds to data taken on 256×256 lattices (averaged over 60 initial conditions), and ◇ corresponds to data taken on 128×128 lattices (averaged over 60 initial conditions). Statistical fluctuations are shown whenever larger than the symbol size.

Another length scale, which we have considered, is $\lambda_1(t)$, the inverse of the first moment of the circularly averaged scattering function. Each associated domain (of size λ_1) spans over 15–20 vortices (λ_1^2/d^2) so that in measuring its average orientation the single-vortex field configurations are, to some extent, averaged out. The $\bar{k}_1$ moment gives us information on the large-scale relaxation processes. These involve rearrangements of the vortex-field configurations that can take place even in the absence of vortex annihilations. In our largest ($L=512$) and longest (up to 6400 time steps) simulations, $\bar{k}_1^{-2}$ behaves linearly for all $t>1000$, as shown in Fig. 3. A small deviation at early times can be observed, but this is substantially less pronounced than for $\bar{k}_2^{-2}$. This seems to indicate that the large-scale relaxation processes do in fact follow the usual 1/2 power law found in nonconserved systems. Analogous behavior is found for $r_{1/2}^2$, but our data for this quantity only extends up to 3200 time steps.

The first moment of the circularly averaged scattering function reflects the behavior of the long-wavelength fluctuations in the system and is therefore much more sensitive to finite-size effects than $\bar{k}_2$. In Fig. 3 we have also plotted, for comparison, the calculated averages of $\bar{k}_1$ for smaller systems. The scatter in the data is evident (com-

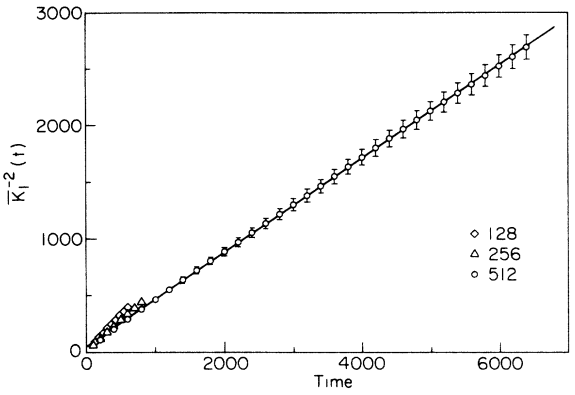

FIG. 3. Inverse of average wave-number square $\bar{k}_1^{-2}$ vs t. For the interpretation of the symbols see Fig. 2. We also show the statistical fluctuations and the best linear fit to the data taken on 512×512 lattices.

pare the same averages for $\bar{k}_2$ in Fig. 2). This suggests that $\bar{k}_1$ might be an appropriate quantity to exhibit finite-size scaling (see below).

Another important distinction between the $\bar{k}_2$ and $\bar{k}_1$ moments is the character of their fluctuations. The value of the second moment at any given time is a self-averaging quantity while the value of the first moment is not self-averaging. This means that if we take the average of $\bar{k}_2(t)$ over the same number of initial conditions for two systems of linear size L and $2L$, respectively, in $D=2$, the observed standard deviation of $\bar{k}_2$ in the larger system will be reduced by a factor of $1/2$ with respect to standard deviation in the smaller system. On the other hand, the standard deviation for $\bar{k}_1$ will only decrease by a factor of about $1/\sqrt{2}$. The reason for this discrepancy is again the different relative weights given to the small-k components of the scattering function in the two cases.

IV. VORTEX DYNAMICS

In order to gain some insight about the long transient observed during the first 1500 updates, we have considered the possible role of the charge fluctuations in the initial distribution of vortices and antivortices. In two dimensions, these charge fluctuations can be significant, and could potentially account for the long transient. Nevertheless, as we show below, this interesting possibility does not seem to occur, at least in the simplest form that we have considered.

If vortices and antivortices at $t=0$ were distributed at random, the density fluctuations $\delta\rho(t)$, in a planar domain of linear dimension R, would be proportional to $\sqrt{\rho(0)R^2}$ $[d(0)<R<L]$, where $\rho(0)$ is the initial average vortex density and $d(0)$ is the initial intervortex spacing. In the present system the initial distributions for vortices and antivortices must satisfy Stoke's theorem: the field vorticity on a domain boundary is equal to the topological charge imbalance (fluctuation) in the domain.[23] This implies that the initial fluctuations will scale with the linear dimension R (perimeter) of the domain as $\sqrt{\rho(0)d(0)R}$. We have numerically verified that this scaling relation is satisfied in our system also at later times, for $d(t)<R<L$.

We now relate this result to the dynamics of the system. Since the annihilation process preserves the local net charge, at time t the number of surviving charges in the system should be proportional to the initial charge fluctuation in a domain size of the order of the diffusion length of vortices. This domain size, $l(t)\sim t^{1/2}$, so that

$$\delta\rho(t)\sim\{\rho(0)d(0)[l(t)]^{D-1}\}^{1/2}/[l(t)]^D ;$$

for $D=2$, $\delta\rho(t)\sim t^{-3/4}$. Thus, we obtain $N(t)\propto t^{-3/4}$ and $\phi=3/8$, as found in the simulation. At late times, we expect that long-range forces (present in our system) will tend to smooth out the initial fluctuations with a corresponding crossover to mean-field behavior.[24] The crucial assumptions in the preceding argument are that the system is, from the very beginning, in a scaling regime, although not necessarily the asymptotic one, and that the vortices do in fact diffuse.

To test this latter hypothesis we have performed an extensive study of the motion of the vortices on the lattice. The main result is presented in Fig. 4, where we show that the mean vortex displacement in the time range $(30<t<1630)$ follows a power-law behavior $l(t)\sim t^{3/8}$. The subdiffusive movement of the individual vortices appears to be incompatible with our preceding argument. This seems, therefore, to exclude a predominant role of

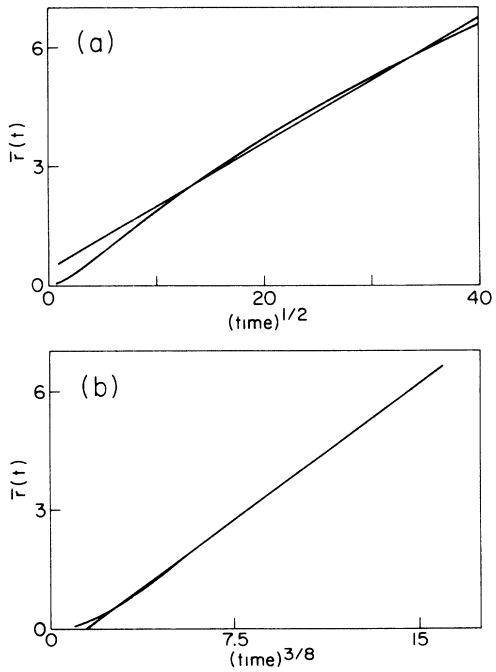

FIG. 4. Average displacement per vortex $\bar{r}(t)$ vs $t^{1/2}$ (a) and $t^{3/8}$ (b). Best linear fits are also shown. $r(t)$ represents the displacement of a vortex with respect to the position it had 30 time steps following the initial quench. The origin of the t axis is chosen here to be equal to the number of times steps minus 30 so that $r(0)=0$. The average is taken over all surviving vortices at time t and we further average over 86 initial conditions.

the charge fluctuations (that is, of a global topological constraint) in slowing down the annihilation process, and it suggests that the observed transient might be related to the dynamics (and therefore to the local environment) of each vortex.

We have also considered the effect of free-boundary conditions on the initial vortex decay. In this case, while the initial decay exponent (3/8) remains unchanged, the average number of vortices present at any given time in the system is somewhat smaller than in the case with periodic boundary conditions. Comparing the results for systems of different size we can see that this effect is due to a "depletion layer" at the system boundaries and that the layer depth grows as the average intervortex spacing. No new length scale is introduced in the system.

With regard to the late-time effects mentioned in Sec. III, we point out that at late times the intervortex interaction is rather weak and pinning effects of vortices on the lattice could play a role in the dynamics of the system, particularly in the absence of thermal noise. We have not attempted to extend the study of the vortex motion to this late stage.

V. FINITE-SIZE AND DYNAMICAL SCALING

In order to verify that the results of Sec. III did not arise from the finite size L of our systems, we performed a scaling analysis of the data. In general, the scattering function can be written

$$S(k,t,\xi,L)=[\bar{k}(t)]^{-2}f(k/\bar{k}(t),\xi\bar{k}(t),L\bar{k}(t)) \ . \quad (5.1)$$

In the large-L limit we must recover the universal curve; assuming that ξ is not a dangerous irrelevant variable, it may be neglected (valid for a deep quench) to obtain from Eq. (5.1) the finite-size scaling relation[25]

$$S(k,t,L)=L^2\Phi_s(kL,L\bar{k}(t)) \ . \quad (5.2)$$

We rescaled the data from our three largest simulations ($L=128,256,512$) using the calculated value of $\bar{k}_1(t)$ corresponding to the largest time-dependent length scale measured in our system, so that there were no free parameters in our procedure. Results for different values of $\bar{k}_1 L$ are shown in Fig. 5; the finite-size scaling relation appears to be obeyed.

We have also tested the scaling relation, Eq. (1.1), and the corresponding relation for $C(r,t)$. We have used $\lambda_2(t)$ as the rescaling length for the scattering function. The associated $\bar{k}_2(t)$ corresponds to the ordinary definition of $\bar{k}$ for a circularly symmetric $S(\vec{k},t)$ in $D=2$. The results for the dynamical scattering function are shown in Fig. 6. They compare favorably with the analogous results for the Ising case. At later times, scaling is satisfied over a larger range of the rescaled $k/\bar{k}_2(t)$ variable, indicating a tendency of the rescaled scattering function to approach the universal master curve $\Phi(x)$. Qualitatively, we can identify three regions in the $k/\bar{k}_2(t)$ dependence of the rescaled scattering function. At very long wavelength $[k/\bar{k}_2(t)<1]$ the scattering function is well approximated by a Gaussian; up to a normalization factor, the same Gaussian fits the data for the

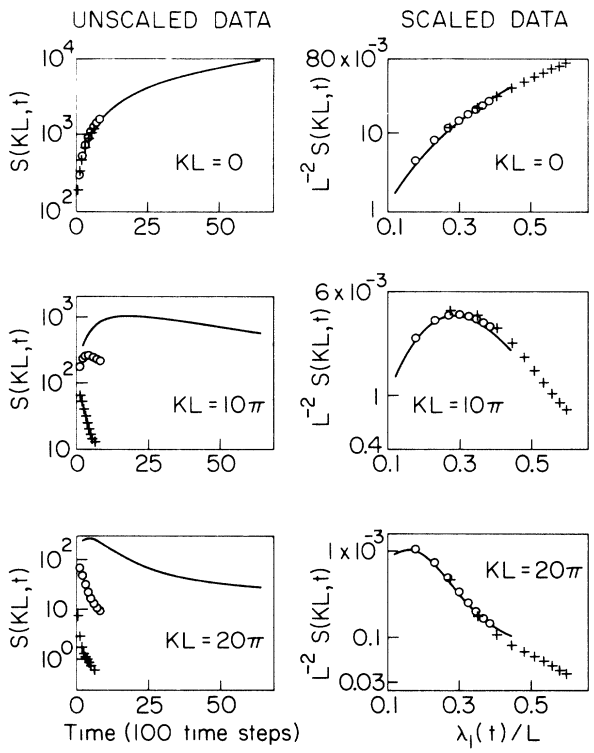

FIG. 5. Demonstration of finite-size scaling for the scattering function, at different values of kL. The solid line corresponds to 512×512 lattices, ○ corresponds to 256×256 lattices, and + corresponds to 128×128 lattices. The data spans three orders of magnitude on the Y axis and it is shown for clarity on a logarithmic scale.

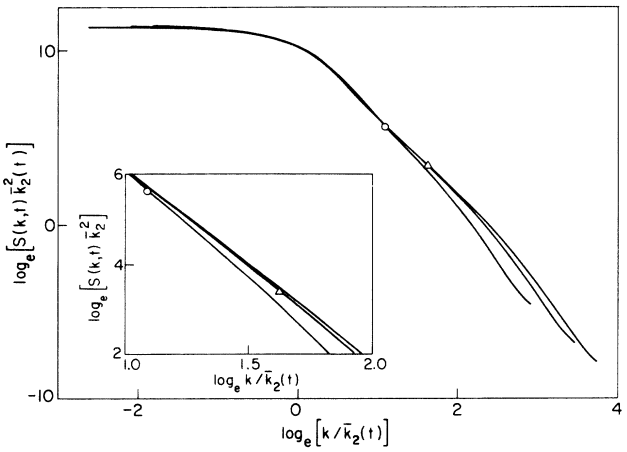

FIG. 6. Graph of $\log_e \bar{k}_2(t)^2 S(k,t)$ vs $\log_e k/\bar{k}_2(t)$ for lattices of size 512×512 at 200, 800, and 1600 time steps. Also plotted are the data for lattices of size 256×256 at 200 and 800 time steps. The data from these different lattices superimpose. The ○ and △ indicate roughly the breakdown of the scaling region for the $t=200$ and 800 curves, respectively, which in both cases occurs when $\lambda \sim 12.5$ lattice spacings. The vortex-core size is roughly eight lattice spacings.

two largest simulations.

The Gaussian behavior breaks down at wavelengths shorter than the typical wavelength $\lambda_2(t)$. This is not surprising, since a characteristic single-vortex field configuration can be seen around each vortex extending to distances comparable with the intervortex spacing. The Fourier spectrum of a (single-) vortex field configuration decays as k^{-2}; this introduces a power-law-bounded correction ($\sim k^{-4}$) in this intermediate wavelength region of the scattering function, where scaling still applies.

At wavelengths comparable to the vortex-core size ξ or shorter, scaling breaks down. The vortex-core size is a time-independent length in the system so that any effect of the vortex core on the rescaled scattering function will disappear in the asymptotic limit [$\xi\bar{k}(t)\to 0$]. The domain-wall thickness gives a similar nonuniversal correction in the Ising case.[26]

To rescale $C(r,t)$, the real-space correlation function of the order parameter, we have used its time-dependent halfwidth $r_{1/2}(t)$. The results are presented in Fig. 7. We have also considered the small x [$\equiv r/r_{1/2}(t)$] limit of the rescaled correlation function $\Gamma(x(t))=C(r,t)$. As shown in the inset of Fig. 7, we find that $\Gamma(x)\approx 1-x^{\psi}$, where $\psi=1.6\pm 0.05$. As expected, $\psi>1$ because of the smooth boundaries, and Porod's law is violated in this system;[26] on the other hand, the fact that $\psi<2$ again points to the presence of nontrivial correction to the Gaussian behavior at short distances. A Gaussian form for the rescaled correlation function is found in models with continuous symmetry, which ignore the presence of vortices.[4,5,16]

We have also considered the real-space correlation functions of the vortices. The radial correlation function for vortices of equal sign is shown in Fig. 8, and the correlation function for vortices of opposite sign is shown in Fig. 9. These distributions should go to zero at distances comparable to, or smaller than, the vortex core. In practice we chose one lattice spacing as the minimal intervortex distance. Over distances comparable with the average intervortex spacing, the behavior of the two correlation functions is, as expected, drastically different, reflecting the role of the intervortex potential. The corre-

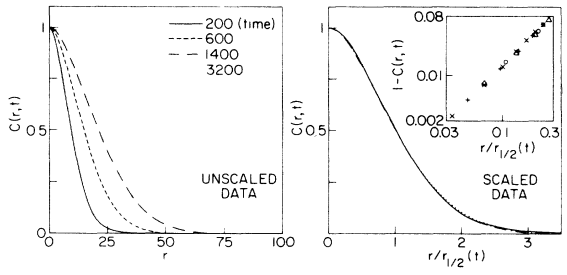

FIG. 7. Demonstration of dynamical scaling for $C(r,t)=\Gamma(r/r_{1/2}(t))$, where $r_{1/2}(t)$ is the halfwidth of $C(r,t)$. We plot data for lattices 512×512 at 200 (solid line, ○), 600 (dashed line, △), 1400 (chain dotted line, +) and 3200 (dotted line, ×) time steps. Inset is a log-log plot of $1-\Gamma(x)$ in the limit of small x. The diagonal of the inset square has a slope of 1.6.

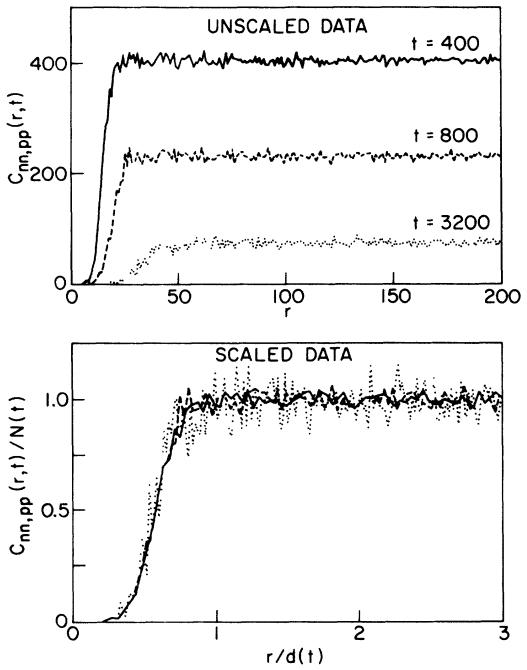

FIG. 8. Demonstration of dynamical scaling for $C_{nn,pp}(r,t)\equiv\langle n(0,t)n(r,t)+p(0,t)p(r,t)\rangle$, where n and p are the (time-dependent) local densities of negative and positive vortices, respectively. $N(t)$ is the total number of vortices in the system at time t and $d(t)=L/\sqrt{N(t)}$. The data were taken on 512×512 lattices at 400 (solid line), 800 (dashed line) and 3200 (dotted line) times steps. We averaged over 58 initial conditions.

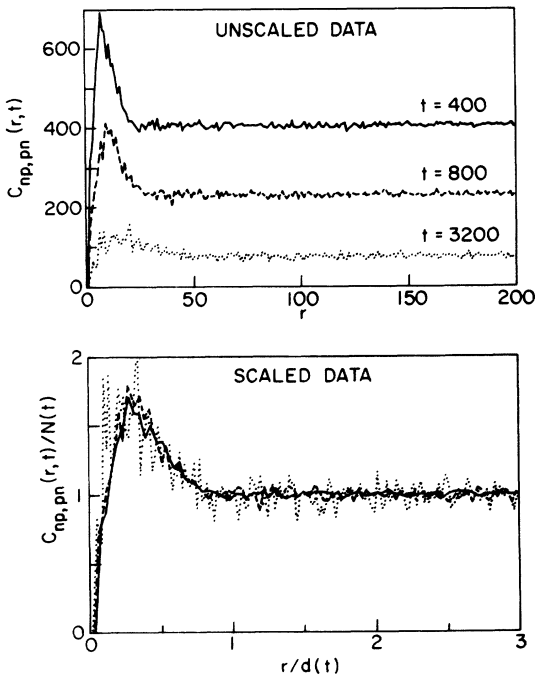

FIG. 9. Demonstration of dynamical scaling for $C_{np,pn}\equiv\langle n(0,t)p(r,t)+p(0,t)n(r,t)\rangle$. Here we have adopted the same symbols and conventions of Fig. 8.

lation functions flatten out for distances larger than one average intervortex spacing $d(t)$, which can therefore be identified with the time-dependent intervortex correlation length. This should be contrasted with the bulk correlation length of the order parameter, which is time independent and characterizes the size of the vortex core. We have used $d(t)$ as the natural rescaling length for the correlation functions. As shown in Figs. 8 and 9, a reasonable scaling behavior is observed from early times, but at late times the noise in the data makes a quantitative comparison more difficult.

VI. COMMENTS AND CONCLUSIONS

Our simulation is, strictly speaking, a zero-temperature simulation. If we wait long enough our system will reach one of the (infinitely) degenerate uniform ground states, chosen by the (random) initial condition. As is well known, in $D=2$ at nonzero temperature T, such a uniform ground state is unstable against spin wave excitations. This process can also be described in related models with continuous symmetry in terms of the macroscopic diffusion of the "phase" field.[27]

Let us briefly discuss how our results might be modified for $T>0$. An important point for our simulations is that at low temperatures the characteristic decay time t_0 of the ground state becomes extremely large, and it grows as the area (L^2) of the system. In practive, for a typical noise amplitude ≈ 0.1 of the equilibrium modulus length of the order-parameter vector and $L>32$, t_0 greatly exceeds the typical observation time scale of our simulations. The observation time scale corresponds to the characteristic time-dependent length scale $\lambda(t)$ becoming of the order of the system size L. At low temperature, for very large system sizes, our results will describe the initial relaxation of the system controlled by the intervortex interaction while the thermal noise will dominate the evolution of the system at later times, destabilizing the increasingly large vortex-free regions. Such a physical picture should also hold in three dimensions for systems of finite size below the ordering transition temperature. The crucial difference, as seen in the $n=\infty$ case,[27] is that in $D=3$ the characteristic time for "phase diffusion" τ_p increases as L^3, which is much faster than any other relaxation time τ in the system (at most L^2). Thus the ratio τ_p/τ diverges with increasing system size and the broken-symmetric ground state becomes stable in the thermodynamic limit.

In summary, we have shown that the vortex annihilation dynamics significantly affects the initial ordering process of a system with a continuous symmetry. Even in this transient regime, all the correlation functions we have considered appear to satisfy dynamical scaling. Finite-size scaling of the scattering function is also satisfied. We have observed departures from Gaussian behavior of the correlation functions. This deviation appears to be related to the presence of vortex configurations extending over distances comparable to the average intervortex spacing. The value of the dynamical exponent seen in the late stages of our simulations is consistent with $\phi=1/2$; but of course, we cannot rule out further changes in the effective exponent ϕ at times larger then 6400. In particular, the small but measurable differences in the behavior of different representative length scales leave open some questions regarding the true asymptotic nature of the regime investigated. If our numerical results are taken at face value, then it appears that the kinetic coefficient is not renormalized, in contrast to the situation for the critical dynamics of model A. We are presently studying the relaxation dynamics of a system with continuous symmetry and conserved order parameter. The results of this work are planned to be presented in a forthcoming paper.

ACKNOWLEDGMENTS

We thank Yoshi Oono for a number of valuable discussions. This work was supported partially by the National Science Foundation through Grant No. DMR-89-20538 administered through the Illinois Materials Research Laboratory. We acknowledge the support of the Computer Center at the Material Research Laboratory and the use of the CRAY X-MP/48 at the National Center for Supercomputing Application at the University of Illinois at Urbana-Champaign. One of us (N.D.G.) gratefully acknowledges the support of the Alfred P. Sloan Foundation.

[1]General overviews of the field can be found in H. Furukawa, Adv. Phys. **34**, 703 (1985); J. D. Gunton, M. San Miguel, and P. S. Sahni, in *Phase Transitions and Critical Phenomena*, edited by C. Domb and J. L. Lebowitz (Academic, New York, 1983), Vol. 8.

[2]B. D. Gaulin, S. Spooner, and Y. Morii, Phys. Rev. Lett. **59**, 668 (1987); R. Toral, A. Chakrabarti, and J. D. Gunton, Phys. Rev. Lett. **60**, 2311 (1988).

[3]K. Kawasaki and T. Ohta, Physica A **118**, 175 (1983), and references therein.

[4]G. F. Mazenko and M. Zannetti, Phys. Rev. B **32**, 4565 (1985).

[5]F. de Pasquale and P. Tartaglia, Phys. Rev. B **33**, 2081 (1986).

[6]H. Toyoki and K. Honda, Prog. Theor. Phys. **78**, 273 (1986).

[7]K. Kawasaki, Phys. Rev. A **31**, 3880 (1985), and references therein.

[8]H. Nishimori and T. Nukii, J. Phys. Soc. Jpn. **58**, 563 (1989).

[9]H. Toyoki, in *Dynamics of Ordering Processes in Condensed Matter*, edited by S. Komura and H. Furukawa (Plenum, New York, 1988).

[10]A. J. Bray, Phys. Rev. Lett. **62**, 2841 (1989).

[11]P. C. Hohenberg and B. I. Halperin, Rev. Mod. Phys. **49**, 435 (1977).

[12]A. J. Bray, Phys. Rev. B **41**, 6724 (1990).

[13]N. Goldenfeld and Y. Oono (unpublished).

[14]The results for the conserved order-parameter case will be presented elsewhere.

[15]H. Toyoki and K. Honda, Phys. Rev. B **33**, 385 (1986). This result is true for random initial configurations [$\langle \psi(0) \rangle = 0$].

When $\langle \psi(0) \rangle \neq 0$ the relaxation dynamics becomes exponential. An analysis of the same effect in our system will be given elsewhere.

[16]T. J. Newman, A. J. Bray, and M. A. Moore (unpublished).

[17]Y. Oono and S. Puri, Phys. Rev. Lett. **58**, 836 (1987); Phys. Rev. A **38**, 434 (1988); A. Chakrabarty and J. Gunton, Phys. Rev. B **37**, 3798 (1988); Y. Oono and M. Bahiana, Phys. Rev. Lett. **61**, 1109 (1988).

[18]1/3 is, in fact, the probability that an elementary lattice square encloses a nonzero flux. This can be calculated as the probability that the sum of three random angles (uniformly distributed between $-\pi$ and π) will add up to an absolute value greater than π.

[19]All our measurements involve an ensemble averaging over initial conditions and, for space- or wave-vector-dependent quantities, an average over all directions.

[20]The fact that $\lambda_2(t) < 2d(t)$ indicates some degree of dimerization in the system: vortices of different charge are closer on average than vortices of equal sign; this shows up directly in the corresponding correlation functions.

[21]We note that the early times behavior of $\lambda_2(t)$ and $d(t)$ ($\sim t^{3/8}$) agrees with the result of the $D=3$ study of Nishimori and Nukii reported in Ref. 8. A typical domain size in $D=3$ is given by $[L^3/l(t)]^{1/2}$, where L is the size of the sytem and $l(t)$ ($\sim t^{-0.75}$) is the total length of the vortex lines.

[22]S. Puri and Y. Oono, Phys. Rev. A **38**, 1542 (1988).

[23]From this immediately follows that, when we apply periodic boundary conditions, the net charge in the system is zero at all times.

[24]D. Toussaint and F. Wilczek, J. Chem. Phys. **78**, 2642 (1983); T. Ohtuski, Phys. Lett. **106A**, 224 (1984); K. Lee and E. J. Weinberg, Nucl. Phys. **B24**, 354 (1984).

[25]J. Viñals and D. Jasnow, Phys. Rev. B **37**, 9582 (1988); Mod. Phys. Lett. B **2**, 527 (1988).

[26]Y. Oono and S. Puri, Mod. Phys. Lett. B **2**, 861 (1988).

[27]F. de Pasquale, Z. Racz, and P. Tartaglia, Phys. Rev. B **28**, 2582 (1983). See also Ref. 5.